12-2012

# Creating the park cool island in an inner-city neighborhood: Heat mitigation strategy for Phoenix, AZ

Juan DECLET-BARRETO

Anthony J. BRAZEL

Chris A. MARTIN

Winston T. L. CHOW
*Singapore Management University*, winstonchow@smu.edu.sg

Sharon L. HARLAN

Urban Ecosyst (2013) 16:617–635
DOI 10.1007/s11252-012-0278-8

# Creating the park cool island in an inner-city neighborhood: heat mitigation strategy for Phoenix, AZ

**Juan Declet-Barreto · Anthony J. Brazel · Chris A. Martin · Winston T. L. Chow · Sharon L. Harlan**

Published online: 21 December 2012


**Abstract** We conducted microclimate simulations in ENVI-Met 3.1 to evaluate the impact of vegetation in lowering temperatures during an extreme heat event in an urban core neighborhood park in Phoenix, Arizona. We predicted air and surface temperatures under two different vegetation regimes: existing conditions representative of Phoenix urban core neighborhoods, and a proposed scenario informed by principles of landscape design and architecture and Urban Heat Island mitigation strategies. We found significant potential air and surface temperature reductions between representative and proposed vegetation scenarios: 1) a Park Cool Island effect that extended to non-vegetated surfaces; 2) a net cooling of air underneath or around canopied vegetation ranging from 0.9 °C to 1.9 °C during the warmest time of the day; and 3) potential reductions in surface temperatures from 0.8 °C to 8.4 °C in areas underneath or around vegetation.

**Keywords** Microclimate simulation · Heat island · Urban vegetation · Heat wave · Phoenix · Park cool island

**Electronic supplementary material** The online version of this article (doi:10.1007/s11252-012-0278-8) contains supplementary material, which is available to authorized users.

J. Declet-Barreto (✉) · S. L. Harlan
School of Human Evolution and Social Change, Arizona State University, P.O. Box 872402, Tempe, AZ 85287-2402, USA
e-mail: juan.declet@asu.edu

A. J. Brazel
School of Geographical Sciences and Urban Planning, Arizona State University, P.O. Box 875302, Tempe, AZ 85287, USA

C. A. Martin
Department of Applied Sciences and Mathematics, Arizona State University, 6073 South Backus Mall, Mesa, AZ 85212, USA

W. T. L. Chow
Department of Engineering, College of Technology and Innovation, Arizona State University, 7231 E Sonoran Arroyo Mall, 330 Santan Hall, Mesa, AZ 85212, USA

## Introduction

Urban climate research has empirically established spatio-temporal relationships between land cover and heat fluxes in cities, and is especially attentive to Urban Heat Islands (UHIs) in cities (Mills 2006; Roth 2002; Voogt and Oke 2003). The climatic consequences of anthropogenic surface cover changes at the regional scale are well understood. The replacement of natural covers with the urban fabric results in significantly higher nighttime temperatures in built-up areas compared to the surrounding rural environment (Balling and Brazel 1987; Lowry 1967; Oke 1997). Reintroducing urban green spaces with canopied vegetation can alter surface and near-surface energy flows and act as wind tunnels or barriers, potentially reducing the intensity of UHIs (Barradas et al. 1999; Grimmond et al. 1996; Oke 1989). There are two principal ways in which vegetation influences surface energy flows that in turn affect surface and near-surface temperatures. Larger plants such as trees attenuate radiant energy flows through absorption and reflection. Less radiant energy contacting the ground surface reduces surface and near-surface temperatures. This microclimate ecosystem service is known as shading. The second mechanism is related to plant consumption of energy during transpiration. As water is evaporated from a liquid to a gas at the surface of cellular structures inside leaves, temperature reductions occur in the immediate environment surrounding a leaf. We refer to this microclimate ecosystem service as transpirational cooling.

One way to study these ecosystem services is by examining the Park Cool Island (PCI). The PCI is an irregular pattern of cooler areas nested within generally warmer urban areas, created by shading and transpirational cooling and extended to the air above non-vegetated areas through advective cooling (Chow et al. 2011). Creating the PCI by increasing vegetation is an increasingly studied strategy for mitigating the effects of the UHI. Numerical modeling of the PCI at the microscale is a valuable tool to explore vegetation modification and its effects on microclimate cooling, especially in areas where energy flux interactions among canopied vegetation and impervious surfaces at a fine scale are not well documented.

The purpose of our study was to evaluate the role of vegetation in creating the PCI in a sparsely-vegetated, low-income, ethnic minority community in inner-city Phoenix, Arizona. We modeled air and surface temperatures to better understand the role of vegetation in providing shading and transpirational cooling as a strategy for moderating the UHI. We conducted microclimate simulations in ENVI-Met, a three-dimensional prognostic simulation of surface-plant-air energy interactions (Bruse and Fleer 1998). The modeling system solves a series of differential equations to simulate processes of surface heat, vapor and vegetation exchange, vertical surface air flows, particle dispersion, turbulence, and bioclimatology.

We used ENVI-Met to simulate the PCI during an extreme heat event (EHE). EHEs are characterized by sustained periods of high temperatures above the range of normal variability (IPCC 2007; Meehl and Tebaldi 2004). For the duration of the EHE, we predicted air and surface temperatures within the park at the microscale (modeling cell size = 3.59 × 1.00 m). We first modeled the 24-hour profile of predicted surface and air temperatures by surface cover type for representative existing park vegetation conditions compared to an alternative proposed park landscape design with more vegetation. Second, we examined the spatial distribution of temperature differences between the representative existing and proposed vegetation conditions, and estimated the extent of the potential PCI. We contribute to urban ecology research by evaluating the relationships among vegetation, ecosystem services, and the PCI with microclimate modeling and by applying a spatial analysis technique to mapping the PCI.

## Vegetation and extreme heat mitigation in Phoenix

Mitigating high temperatures in desert cities like Phoenix, where the weather is chronically hot for half of the year and EHEs occur frequently in the summer, is an important policy goal. Mesoscale climate modeling and analyses of historical temperature data in metropolitan Phoenix have shown that both the severity and extent of UHIs continue to increase, especially in the urban core (Grossman-Clarke et al. 2005; Ruddell et al. 2010). Indeed, Maricopa County (where metropolitan Phoenix is located) experienced an increase in average temperature of more than 3 °C during the 20th century, while temperatures in Arizona's urban areas increased at three times the rate of regional temperature increase (Brazel et al. 2000) . Heavily built-up urban areas like Phoenix are expected to experience more—and more severe—extreme heat events and longer warm seasons throughout the 21st century (Diffenbaugh et al. 2005). Extreme heat is a threat to human health, increases atmospheric pollutants and energy and water use, alters regional hydrology, and impacts interactions between humans and ecological processes (Anderson and Bell 2011; Brazel et al. 2007; Jenerette et al. 2007; Wolf et al. 2010).

Recent research in metropolitan Phoenix stresses the critical role of vegetation in mitigating high temperatures in desert cities. Ruddell et al. (2010), for example, found that Phoenix neighborhoods with higher vegetative densities had significantly lower temperatures during an EHE than those with xeric or sparse vegetation. Stabler et al. (2005) studied relationships of vegetated land cover (expressed as NDVI) with land use, air temperature, and humidity, and found that microclimates in Phoenix are caused by heat flux interactions between vegetation and non-vegetated surfaces. Similarly, Jenerette et al. (2007) combined remotely-sensed surface temperature and vegetated land cover (NDVI) at the scale of U.S. census tracts and found a statistically significant correlation between sparse vegetation and high temperatures. Desert cities like Mexicali (Baja California, México) also show significant intra-urban land cover-dependent variability in the composition and intensity of the UHI (Garcia-Cueto et al. 2007). A study in Cairo, Egypt found a distinct nocturnal heat island effect during the warm season, associated with land cover: urban areas had drier and warmer atmospheric conditions compared to rural or suburban parts of the city (Robaa 2003).

## Social dimensions of green spaces (parks) in urban areas

The association of temperature and vegetation with ethnicity and socioeconomic status is also well documented in urban ecology and social science research in Phoenix. Some research has been especially attentive to weather conditions that expose humans to the effects of heat stress. Heat stress, which is a threat to human health and can cause severe illness or death (EPA 2011), is triggered when temperature thresholds of human tolerance are exceeded. Harlan et al. (2006) found that low-income, minority neighborhoods in Phoenix were warmer and more sparsely vegetated than higher-income, predominantly white neighborhoods and consequently residents were more exposed to temperatures that cause heat stress. Multivariate modeling of the entire metropolitan area by Jenerette et al. (2007) found a positive statistical relationship between neighborhood affluence and more vegetated land cover. In Phoenix, economic stratification in access to vegetation-based ecosystem services is a relatively recent phenomenon, which was not present in the 1970s, but clearly increased each decade through 2000 (Jenerette et al. 2011). Buyantuyev and Wu (2012) found that although surface temperatures in Phoenix are driven largely by vegetation and impervious surface distributions, median family income mediates this relationship. Together, these studies suggest that green spaces have desirable ecological outcomes in Phoenix but low-

income communities are receiving fewer benefits and the gap between higher- and lower-income neighborhoods is increasing over time.

In addition to the demonstrated impacts of vegetation on UHI mitigation, green spaces provide other ecosystem services, such as reduction of airborne contaminants, absorption of rainfall, buffering against flooding, and habitats for wildlife (Boone et al. 2009; Currie and Bass 2008; de Groot et al. 2010; Payne-Sturges et al. 2006). These ecosystem services play a role in creating "salutogenic" urban environments that can help mitigate human health problems, such as asthma, allergies, obesity, and increased stress. It has been shown that lack of green spaces in cities contributes to health disparities among people in lower- and higher-income neighborhoods (Jennings et al. 2012; Wilson 2009). Public outdoor heat mitigation strategies in parks and other public spaces are especially needed in socially and ecologically vulnerable areas of cities because residents in these areas have fewer household social and economic resources to adapt their microscale outdoor and indoor environments to extreme heat (Harlan et al. 2006; Martin et al. 2004).

Studies focused on environmental equity find that both the quantity and quality of parks are unevenly distributed within cities, and that low-income and minority communities sometimes have less access to such amenities (Boone et al. 2009; Byrne et al. 2009). Research in this field combines urban socio-ecological and historical perspectives to argue that intra-city disparities in the location of quality parks are the outcome of complex interactions between cultural, ecological, and political processes that continuously reshape urban environments and differentially benefit socio-economically advantaged populations at the expense of poor or low-income communities (Brownlow 2006; Dooling et al. 2006). The provision of ecologically adequate—and adequately maintained—vegetation is important for equitable outcomes, especially since neglected parks often create "ecologies of fear" that emphasize legacies of race-based social control and criminalization of environments and their occupants (Brownlow 2006).

Increasingly, minority communities argue that the dearth of adequate park facilities is an environmental injustice that demands redress by authorities and city planners. Inequities in park access and ecological conditions can be framed according to intra-city differences in fiscal expenditures for parks infrastructure. In inner-city Phoenix, inadequate parks infrastructure is most evident in lack of grass and tree irrigation, paucity of regular park maintenance by city staff, particulate matter pollution from dirt lots on park grounds, and unbuffered industrial land uses and freeways sited near parks–conditions that prevail in the poorer areas of the city. Therefore, the environmental justice issues related to urban green spaces suggest that vegetation-based UHI mitigation strategies may help address not only extreme heat, but also contribute to achieving a more equitable distribution of ecological services in the city.

## Methods

### Study area

Our study area is the Latino Urban Core neighborhood, a sparsely-vegetated, low-income, ethnic minority neighborhood in the urban core of downtown Phoenix. It is bounded by industrial land uses to the north, south, and east, and by an interstate freeway to the west. As shown in Fig. 1, the portion of the neighborhood in the modeling domain (~3.59 ha in area) currently has little vegetation. A central feature of the neighborhood, as seen in the aerial photo, is an electric utility company easement currently used as a linear park space almost entirely devoid of vegetation. The sparse vegetation in the neighborhood is located mostly in

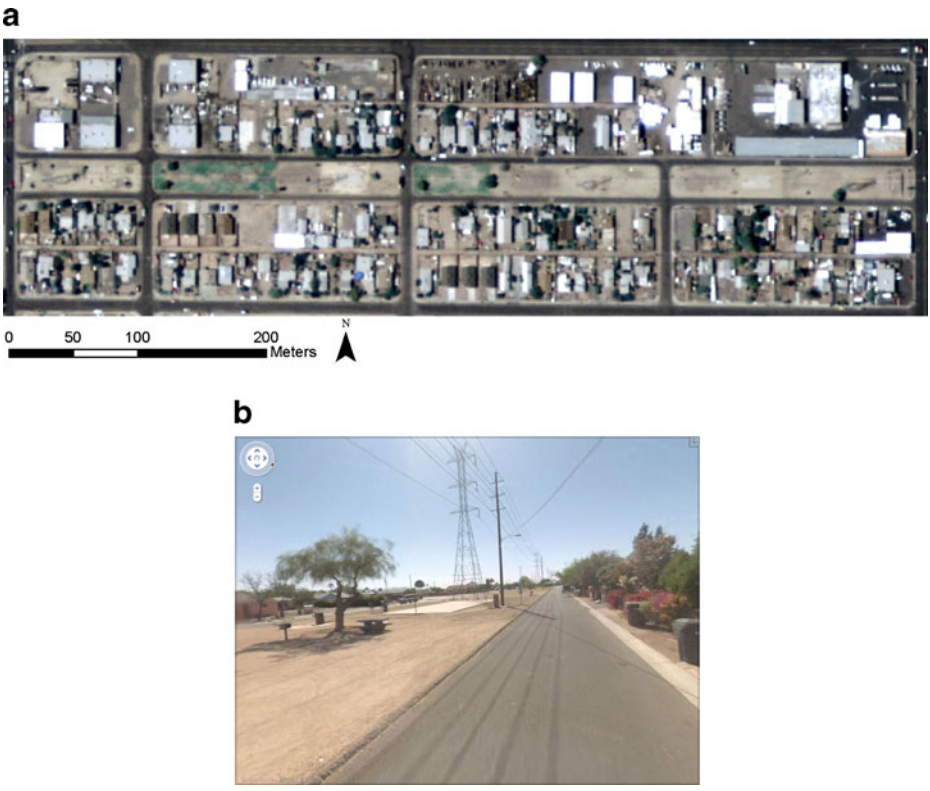


**Fig. 1** **a** The Latino Urban Core (LUC) study area is characterized by a linear park with little vegetation and residential areas unbuffered from industrial land uses. **b** Sparse vegetation, exposed soil, and high-capacity electrical towers typical of the LUC study area. Image source: Google Street View

the front and backyards of residences, and is comprised of both desert and non-native plant species (Table 1). Abundant patches of exposed soil are found throughout the neighborhood in vacant lots, front and backyards, and in the park grounds.

This neighborhood was deemed suitable for modeling the relationship between vegetation and energy fluxes based on previous research in Phoenix that found similar low-income and minority communities were associated with higher temperatures, sparse vegetation, and increased heat stress (Harlan et al. 2006; Jenerette et al. 2007). We focused our analysis on the park and on the industrial and residential blocks immediately north and south of it.

## Microclimate modeling in ENVI-Met 3.1

ENVI-Met is useful for analyzing small-scale impacts of vegetation and rooftops on local microclimates because spatially-explicit thermal data from remote sensing platforms are too coarse for studying intra-urban environments. The highest spatial resolution (pixel size) of available remotely-sensed thermal data ranges from 30 to 90 m (ASTER 2010). Such coarse resolutions render thermal sensor data unsuitable for microclimate investigations, where the influence of individual land covers, trees or other plants, on atmospheric and surface energy fluxes is of interest. We compared the modeled results of air ($T_a$) and surface ($T_s$) temperature for two vegetation scenarios to gauge how differences in vegetation cover would change the

**Table 1** Taxa in LUC study area

| Symbol | Taxonomic name | Common name |
|---|---|---|
| BG | *Cynodon dactylon* | Bermuda Grass |
| SA | *Fraxinus uhdei* | Shamel Ash |
| WM | *Morus alba* | White Mulberry |
| OG | *Muhlenbergia capillaries, Muhlenbergia rigens, Stipa tenuissima*[a] | Pink muhly, deer grass, Mexican thread grass |
| EO | *Olea europaea* | European Olive |
| PV | *Parkinsonia culeata* | Palo Verde |
| MP | *Pinus eldarica* | Afghan Pine |
| TM | *Prosopis hybrid* | Thornless Mesquite |
| AS | *Rhus lancea* | African Sumac |
| CE | *Ulmus parvifolia* | Chinese Elm |
| FP | *Washingtonia filifera* | Desert Fan Palm |
| MP | *Washingtonia robusta* | Mexican Fan Palm |

[a] This type generalizes three grasses into an "ornamental grass" type for ENVI-MET modeling

intensity of a major heat wave's effect on the park. We also mapped a local indicator of spatial autocorrelation to estimate the magnitude and spatial extent of the potential PCI created by differences in air temperature between the scenarios. We relied on validation of simulated temperatures in Chow et al. (2011), which included ENVI-Met modeling and a temperature data collection campaign conducted in a site in metropolitan Phoenix with similar vegetation and microclimate conditions.

The ENVI-Met system divides a study area into equal-sized cells, for which surface and air temperature, air flow, and other indicators are predicted based on user-provided initial atmospheric conditions and urban spatial structure. Microscale models (typically 0.5–10.0 m horizontal resolution) can describe intra-urban variability in microclimatic signatures that are not captured by the coarser resolution (~5–30 km) of mesoscale simulations. ENVI-Met has been applied in European cities to evaluate strategies for UHI mitigation (Huttner et al. 2008), to estimate the cooling effects of green spaces (Lahme and Bruse 2003), and to simulate the localized effects of global warming (Huttner et al. 2008). In studies within metropolitan Phoenix, Ozkeresteci et al. (2003) modeled scenarios to inform urban design and planning strategies and Rosheidat et al. (2008) evaluated strategies to increase pedestrian thermal comfort. Chow et al. (2011) used ENVI-Met to model the role of vegetation in creating the PCI, and Hedquist et al. (2009) modeled an urban canyon near the Phoenix city center. The latter two studies compared their respective simulation results with field-collected surface and atmospheric data, and the models compared well to field observations. Chow et al. (2011) used several difference measure indices (e.g. RMSE and MAE) to evaluate ENVI-Met simulations against observed temperatures and reported reasonable model accuracy of both spatial distribution and time-series of simulated temperature data. Hedquist et al. (2009) found that simulation temperatures compared best to observations during the hours of maximum UHI intensity, typically 3–5 h after sunset.

## Air and surface temperatures

Increases in $T_a$ and $T_s$ are the best understood and most frequently observed indicators of the effects of urbanization in UHIs (Roth 2002). $T_a$ can describe UHIs at the urban canopy layer

(i.e., beneath the general height of buildings or trees, whichever is greater), and is obtained from data 2 m above surface level (a.s.l.) from the ENVI-Met model. $T_s$ is an important UHI indicator because the properties of surface materials and processes associated with them greatly influence the radiative, thermal, and emissions properties of both surfaces and the atmosphere (Roth 2002). In ENVI-Met, $T_s$ is obtained from surface output data.

## Model specification

We modeled temperatures under two distinct vegetation regimes, for which we specified two 200×50×25 cell modeling grids at spatial resolutions of 3.59, 1.00, and 2.00 m for the x-, y-, and z-axes, respectively. The locations of rooftops in the study area are identical in both scenarios, and were specified by overlaying aerial imagery in the ENVI-Met editor software interface and assigning a height of 4 m to residential structures and 8 m to industrial or commercial rooftops. To model vegetation, ENVI-Met 3.1 requires structural characteristics such as stomatal resistance, leaf area density (LAD), and carbon fixation type. Default vegetation types included in ENVI-Met, however, are typical of European temperate forests, and do not adequately characterize vegetation in desert cities like Phoenix. To address this limitation, we conducted a vegetation survey in the study area to generate an ENVI-Met ready plants database that is representative of vegetation in the study area (Table 2). Leaf area indices (LAI) of vegetation found in the study area were measured with a Li-Cor LAI-2000 plant canopy analyzer (http://www.licor.com/). Vertical LAD distributions were estimated for each vegetation species based on the method proposed by Lalic and Mihailovic (2004). As part of the survey, we also obtained GPS coordinates of plants and trees in the park portion of the study area. Taxa of non-grass vegetation on private property or in otherwise inaccessible areas were identified using a combination of fieldwork and Google Maps Street View. We relied on the Virtual Library of Phoenix Landscape Plants (Martin 2009) for visual matching of vegetation species in our fieldwork.

In addition to land surface characterization, the model requires wind speed and direction, relative humidity of the air (RH), and surface roughness ($Z_0$) parameters to initiate the model. We obtained these from the 16 July 2005 (0500 h) record for a nearby PRISM network station ("Kay" site, 33.421° N, 112.151° W, 1,032 fta.s.l.), approximately 4.85 km SW from the study area. Table 3 shows the initial atmospheric, soil, rooftop, and human comfort conditions specified for our 26-hour modeling run beginning 16 July 2005 at 0500 h. Summer 2005 was an extremely hot season in Phoenix. There were 16 instances of record high temperatures and, furthermore, the five-day period 15–19 July of that year constituted the most acute EHE of the season according to Ruddell et al. (2010), using Meehl and Tebaldi's (2004) methodology to identify EHEs. We conducted our modeling run from 16 July 2005 0500 h to 17 July 2005 0700 h. Although we report results for the 24-hour simulation period, we concentrate on the results for 16 July 2005 1700 h and 17 July 2005 0500 h to allow adequate time for model spin-up and stability.

Two scenarios were developed to evaluate the impact of vegetation on mitigating extreme temperatures during a documented EHE in Phoenix during 15–19 July 2005. Area input files from the ENVI-Met 3.1 interface are shown in Fig. 2. Table 4 details the distribution of surface covers in each of the modeling scenarios.

## Scenario 1 – representative vegetation (RV)

For our first scenario, we generated a geospatially-referenced dataset representing the 2007 vegetation distribution from a simplified land cover classification dataset created using

**Table 2** Field-derived plant modeling parameters for ENVI-Met

| Plant | $CO_2$ fixation | Plant type | Min stomatal resistance | Shortwave albedo | Height (m) | Root zone depth (m) | LAD1[a] | LAD2 | LAD3 | LAD4 | LAD5 | LAD6 |
|---|---|---|---|---|---|---|---|---|---|---|---|---|
| BG | C4 | grass | 200 | 0.20 | 0.10 | 0.50 | 0.30 | 0.30 | 0.30 | 0.30 | 0.30 | 0.30 |
| OG | C4 | grass | 100 | 0.20 | 0.75 | 0.75 | 0.30 | 0.30 | 0.30 | 0.30 | 0.30 | 0.30 |
| WM | C3 | deciduous tree | 400 | 0.20 | 9.00 | 2.00 | 3.13 | 3.56 | 3.77 | 3.75 | 3.66 | 3.44 |
| PV | C3 | deciduous tree | 400 | 0.20 | 9.25 | 2.00 | 2.41 | 2.79 | 3.01 | 3.01 | 2.95 | 2.78 |
| AS | C3 | deciduous tree | 400 | 0.20 | 8.25 | 2.00 | 3.87 | 4.28 | 4.39 | 4.35 | 4.22 | 3.93 |
| EO | C3 | deciduous tree | 400 | 0.20 | 8.25 | 2.00 | 2.99 | 3.30 | 3.39 | 3.36 | 3.26 | 3.04 |
| MP | C3 | deciduous tree | 400 | 0.20 | 4.75 | 2.00 | 1.62 | 2.02 | 2.42 | 2.67 | 2.67 | 2.58 |
| CE | C3 | deciduous tree | 400 | 0.20 | 8.50 | 2.00 | 1.34 | 1.55 | 1.67 | 1.67 | 1.64 | 1.55 |
| FP | C3 | deciduous tree | 400 | 0.20 | 10.00 | 2.00 | 0.00 | 0.01 | 0.01 | 0.03 | 0.07 | 0.17 |
| TM | C3 | deciduous tree | 400 | 0.20 | 9.00 | 2.00 | 2.55 | 2.83 | 2.92 | 2.89 | 2.81 | 2.62 |
| MP | C3 | deciduous tree | 400 | 0.20 | 20.00 | 2.00 | 0.00 | 0.00 | 0.00 | 0.00 | 0.01 | 0.02 |
| SA | C3 | deciduous tree | 400 | 0.20 | 12.00 | 2.00 | 2.24 | 2.43 | 2.46 | 2.43 | 2.35 | 2.18 |

| Plant | LAD7 | LAD8 | LAD9 | LAD10 | RAD1[b] | RAD2 | RAD3 | RAD4 | RAD5 | RAD6 | RAD7 | RAD8 | RAD9 | RAD10 |
|---|---|---|---|---|---|---|---|---|---|---|---|---|---|---|
| BG | 0.30 | 0.30 | 0.30 | 0.30 | 0.10 | 0.10 | 0.10 | 0.10 | 0.10 | 0.10 | 0.10 | 0.10 | 0.10 | 0.10 |
| OG | 0.30 | 0.30 | 0.30 | 0.30 | 0.10 | 0.10 | 0.10 | 0.10 | 0.10 | 0.10 | 0.10 | 0.10 | 0.10 | 0.10 |
| WM | 2.97 | 2.04 | 0.51 | 0.00 | 0.10 | 0.10 | 0.10 | 0.10 | 0.10 | 0.10 | 0.10 | 0.10 | 0.10 | 0.10 |
| PV | 2.42 | 1.69 | 0.44 | 0.00 | 0.10 | 0.10 | 0.10 | 0.10 | 0.10 | 0.10 | 0.10 | 0.10 | 0.10 | 0.10 |
| AS | 3.35 | 2.24 | 0.51 | 0.00 | 0.10 | 0.10 | 0.10 | 0.10 | 0.10 | 0.10 | 0.10 | 0.10 | 0.10 | 0.10 |
| EO | 2.59 | 1.73 | 0.40 | 0.00 | 0.10 | 0.10 | 0.10 | 0.10 | 0.10 | 0.10 | 0.10 | 0.10 | 0.10 | 0.10 |
| MP | 2.34 | 1.77 | 0.59 | 0.00 | 0.10 | 0.10 | 0.10 | 0.10 | 0.10 | 0.10 | 0.10 | 0.10 | 0.10 | 0.10 |
| CE | 1.35 | 0.94 | 0.25 | 0.00 | 0.10 | 0.10 | 0.10 | 0.10 | 0.10 | 0.10 | 0.10 | 0.10 | 0.10 | 0.10 |
| FP | 0.52 | 1.70 | 2.96 | 3.00 | 0.10 | 0.10 | 0.10 | 0.10 | 0.10 | 0.10 | 0.10 | 0.10 | 0.10 | 0.10 |
| TM | 2.24 | 1.50 | 0.35 | 0.00 | 0.10 | 0.10 | 0.10 | 0.10 | 0.10 | 0.10 | 0.10 | 0.10 | 0.10 | 0.10 |
| MP | 0.07 | 0.36 | 2.39 | 3.00 | 0.10 | 0.10 | 0.10 | 0.10 | 0.10 | 0.10 | 0.10 | 0.10 | 0.10 | 0.10 |
| SA | 1.84 | 1.20 | 0.26 | 0.00 | 0.10 | 0.10 | 0.10 | 0.10 | 0.10 | 0.10 | 0.10 | 0.10 | 0.10 | 0.10 |

[a] Leaf Area Density ($m^2/m^3$)

[b] Root Area Density

**Table 3** Initial parameters for ENVI-Met simulation runs

| Parameters | |
|---|---|
| Atmosphere | |
| Wind speed 10 m a.s.l. (m/s) | 3.58 |
| Wind direction (degrees) | 246 |
| Roughness Length ($z_0$) | 0.3 |
| Initial Atmospheric Temperature (K) | 305.2 |
| Specific Humidity at 2,500 m a.s.l. ($gH_20$/kg air) | 6 |
| Relative Humidity at 2 m a.s.l. (%) | 25 |
| Building | |
| Inside Temperature [K] | 305.2 |
| Heat Transmission Walls ($W/m^2K$) | 3.0 |
| Heat Transmission Roofs ($W/m^2K$) | 9.0 |
| Albedo (Walls) | 0.2 |
| Albedo (Roofs) | 0.3 |
| Soil | |
| Initial Temperature Upper Layer (0–20 cm) (K) | 300.0 |
| Initial Temperature Middle Layer (20–50 cm) (K) | 300.0 |
| Initial Temperature Deep Layer (below 50 cm) (K) | 300.0 |
| Relative Humidity Upper Layer (0–20 cm) (%) | 50 |
| Relative Humidity Middle Layer (20–50 cm) (%) | 60 |
| Relative Humidity Deep Layer (below 50 cm) (%) | 60 |

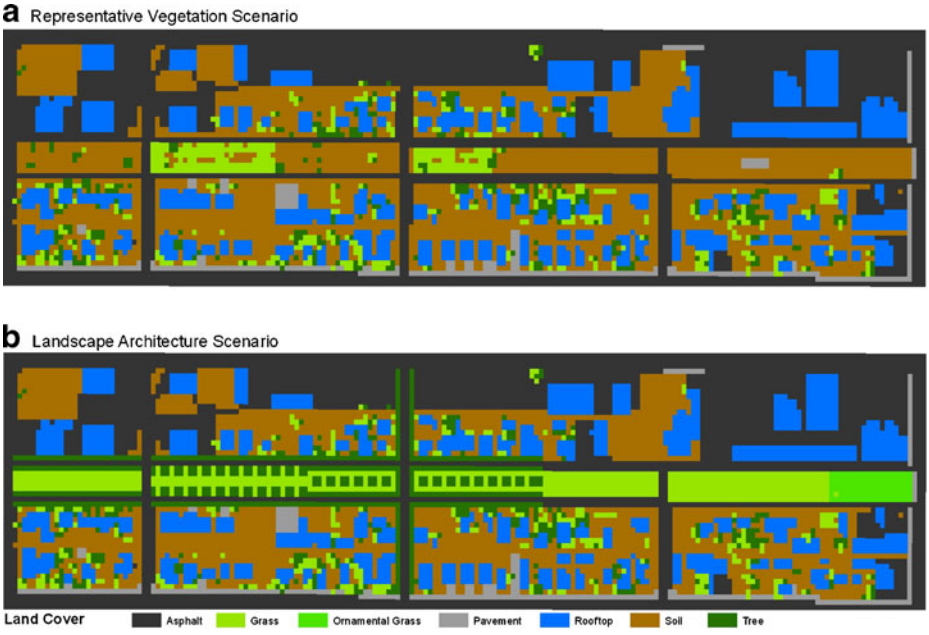


**Fig. 2** ENVI-Met input area files for **a** Representative Vegetation (RV), and **b** Landscape Architecture (LA) modeling scenarios

**Table 4** Number of modeling cells by surface cover class by scenario

| | Representative vegetation (RV) scenario | | Landscape architecture (LA) scenario | |
|---|---|---|---|---|
| Surface cover | *n* | Percent of total area | *n* | Percent of total area |
| Vegetated covers | | | | |
| Bermuda grass | 521 | 5.21 | 992 | 9.92 |
| Ornamental grass | 0 | 0.00 | 107 | 1.07 |
| African sumac | 15 | 0.15 | 0 | 0.00 |
| Afghan pine | 13 | 0.13 | 12 | 0.12 |
| Palo verde | 30 | 0.30 | 15 | 0.15 |
| Shamel ash | 5 | 0.05 | 289 | 2.89 |
| Thornless mesquite | 271 | 2.71 | 565 | 5.65 |
| Non-vegetated covers | | | | |
| Asphalt | 3,740 | 37.40 | 3,604 | 36.04 |
| Loamy soil | 3,359 | 33.59 | 2,387 | 23.87 |
| Pavement | 328 | 3.28 | 311 | 3.11 |
| Rooftop | 1,718 | 17.18 | 1,718 | 17.18 |
| Total | 10,000 | 100.00 | 10,000 | 100.00 |

Object-Based Image Analysis (OBIA), a methodology increasingly used to generate land use/land cover datasets from high-resolution imagery (Hill and Polsky 2007; Walker and Blaschke 2008). We obtained scenes from the 2007 National Agriculture Imagery Program (USD of A 2007) image catalog for Arizona. The generated dataset represents land cover conditions during July 2007, the latest year for which multispectral (RGB plus NIR), high spatial resolution (1 m/pixel) aerial imagery were publicly available. Our land cover classification distinguished trees, grass, and paved roads. It was loaded into the ENVI-Met interface as a raster image and used to assign vegetation and impervious covers to modeling grid cells. Individual species were assigned to modeling cells in ENVI-Met based on the fieldwork and Google Street View method explained above. This scenario was intended to be representative of vegetation typically found in urban core neighborhoods in metropolitan Phoenix.

### Scenario 2 – landscape architecture (LA)

Our second scenario was designed specifically to address UHI mitigation, aesthetic values, and ecological considerations. It also conformed to regulations specific to the land in which the park is located. In consultation with a local landscape architect, we designed a modeling scenario that incorporated both desert and non-native grass and tree species (see Table 1). The park land is a local power company easement with four electrical towers interspersed along the length of the park. Electric utility regulations prohibit the planting of tree species with canopies that could come in contact with overhanging cables and cause electrocution injuries or death. The main danger is that power lines regularly warp under high electrical load conditions. To overcome this limitation, we designed a scenario that placed Arizona mesquite (*Prosopis velutina*) trees within the park (the narrow east–west central band in Fig. 2a, b). Shamel ash (*Fraxinus uhdei*) trees were placed along the residential sidewalks north and south of the park, where there are no limitations related to the electrical transmission towers. Finally, we added ornamental grasses to the eastern end of the park, which is currently dominated by disturbed soil that becomes airborne under windy conditions. The ornamental grass land cover category (see Table 1)

generalized three grassy taxa commonly planted in Phoenix: pink muhly (*Muhlenbergia capillaries*), deer grass (*Muhlenbergia rigens*) and Mexican thread grass *(Stipa tenuissima*).

### Integration of GIS and ENVI-Met 3.1

Our ENVI-Met simulation runs generated a large amount of data. In order to visualize and analyze these data spatially and temporally, we programmed a series of Python-language tools within the geoprocessing framework of ArcMap 9.3 GIS software. These tools allowed us to correlate observations in each grid cell to the surface covers specified in the ENVI-Met area input files. We first programmatically parsed the ENVI-Met area input files for each scenario to generate a GIS polygon vector file (shapefile) with features that corresponded to each of the 10,000 grid cells in the modeling domain, and added each assigned land cover (i.e., tree taxon, grass, soil, rooftop, pavement, asphalt) as tabular data to the shapefile. Because a low number of observations were found for individual tree species (e.g., only 5 shamel ash cells across the RV scenario domain) we assigned all cells containing trees, regardless of taxon, to a generic "tree" class. Upon completion of the two modeling runs, we extracted atmospheric and surface outputs for each of the 26 time steps using the results-extraction tool LEONARDO (packaged with ENVI-Met 3.1) into a flat-file text format. We then used a relational database operation ("join") to correlate observations for each of the two output parameters for each modeling hour to the shapefile representing each modeling scenario. The results are two shapefiles of identical spatial extent (one for each scenario), which are suitable for comparison at each modeling hour time step and throughout the modeling area. For analysis purposes, we eliminated modeling cells containing rooftops because model outputs remained constant throughout the modeling run in these cells.

### Spatial autocorrelation and estimation of the extent of the park cool island (PCI)

We estimated both the potential magnitude and extent of the potential PCI by conducting a cluster analysis on modeled air temperature differences ($dT_a$) using the local indicator of spatial autocorrelation method (LISA, Anselin 1995). LISA is a statistic computed for each observation in a spatial dataset that estimates the degree of significant spatial clustering of values in a variable in neighboring observations. Individual LISA components disaggregate the *global* indicator of spatial autocorrelation, Moran's I, which can be mapped to estimate the degree of *local* spatial autocorrelation within a study area (Anselin 1995; de Smith et al. 2007). The degree of spatial autocorrelation is expressed as a value that indicates the presence of clusters (high or low similar values in proximity, categorized as "high/high" or "low/low" outcomes), or dispersion (no high or low similar values in proximity, categorized as "high/low" or "low/high" outcomes). Computed *p*-values associated with each observation describe the statistical significance of LISA scores. Mapping the high/high outcomes of air temperature differences between the RV and LA ($dT_a$) scenarios provides an estimation of the spatial extent of the potential PCI effect.

## Results

### Diurnal air temperature differences ($dT_a$) and the spatial extent of the park cool island

An ensemble time-series of differences in air temperature ($dT_a$=LA $T_a$ − RV $T_a$) between the two model scenarios over different surface cover types is shown in Fig. 3. Throughout the

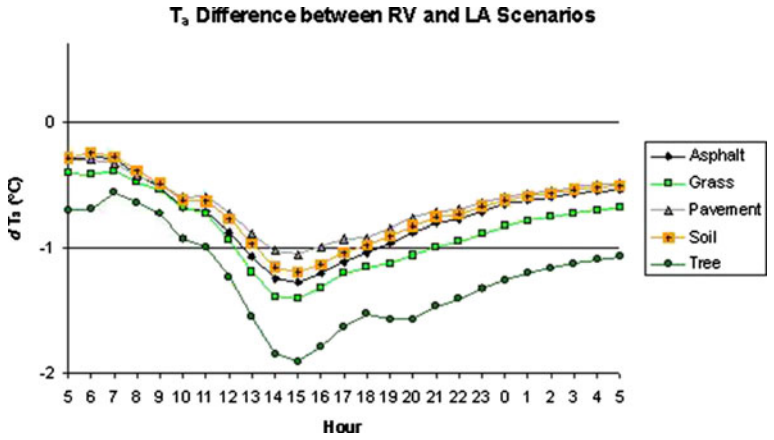


**Fig. 3** 24-hour profile of mean differences in air temperature ($dT_a$) by surface cover between RV and LA scenarios

modeled environment, LA $T_a$ was always lower than RV $T_a$ (negative $dT_a$) over all surfaces throughout the duration of the simulations, with air above the vegetated (tree and grass) and pervious (soil) surfaces showing the most negative $dT_a$. Whereas the most negative $dT_a$ between the two model scenarios occurred in the late afternoon over all surface covers (e.g., ~ −1.9 °C at 1500 h over tree surfaces), negative $dT_a$ between -0.3 °C and −1.3 °C also occurred over all surface cover types post-sunset and persisted until sunrise.

We mapped the spatial distributions of $dT_a$ values for 0500 and 1700 h (Online Resources 1a and 2a). We focused on these two timings because they typically equate to daily minimum and maximum air temperatures, respectively. These maps show significant differences in air temperature ($dT_a$) between the LA and RV scenarios. At 0500 h, $T_a$ reductions typically in the −0.5 to −1.5 °C range occurred around the LA canopied surfaces, whereas the remaining non-canopied and unaltered surfaces experienced modest reductions of up to −0.5 °C (Online Resource 1a). At 1700 h (Online Resource 2a), there were larger $T_a$ reductions around surfaces with canopied vegetation, ranging from −1.0 to −3.1 °C. In addition, remaining impervious and unaltered surfaces experienced cooling in the −0.5 to −1.0 °C range, which was the likely result of greater vegetative evapotranspiration under the LA scenario. Near-surface humidity and latent heat for the entire model domain were higher in the LA scenarios.

We also mapped the potential extent of the PCI according to the calculated $dT_a$ (0500 and 1700 h) between the RV and LA scenarios (Online Resources 1b and 2b). We used modeled $T_a$ as an indicator of the PCI's spatial extent. We estimated the spatial extent of the PCI by calculating a Moran's $I$ statistic, LISA cluster categories, and the statistical significance for each value of $dT_a$ in each cell in the modeling domain.

The Moran's $I$ statistic for $dT_a$ observations indicated a high degree of positive spatial autocorrelation among the grid cells (0.83 at 0500 h, 0.75 at 1700 h, $p<=0.05$), suggesting that, in general, similar values of $dT_a$ are clustered together at both time steps. This global statistic, however, does not describe the spatial distribution of high or low values in the modeling domain, and can, therefore, tell us little about the localized effects of vegetation on air temperatures.

LISA analysis disaggregates Moran's $I$ into the local score calculated for each cell. Statistically-significant clusters ($p<=0.05$) were assigned by the LISA procedure based on

one of four possible outcomes: high/high, low/low, high/low, low/high. Assignment of a cell to either of the first two categories indicates spatial clustering of high or low $dT_a$ at and around that cell. The latter two categories indicate that a cell had a high (low) $dT_a$ surrounded by low (high) values, suggesting no spatial clustering of extreme values around that cell. For our purposes, LISA outcomes of interest were high/high and low/low clusters that represented statistically significant ($p<=0.05$) large $T_a$ differences surrounded by similar large differences or small differences surrounded by similar small differences, respectively.

The high/high outcome indicated that the largest differences of $dT_a$ were spatially clustered, suggesting a cooling effect that followed the pattern of canopied vegetation in the LA scenario (Online Resources 1b and 2b). Clustering of high $dT_a$ values outside modeling cells with canopied vegetation indicated a PCI effect, where the shading and transpirational cooling potential of the canopy extended beyond the location of trees into adjacent areas. The mean $dT_a$ of observations at 1700 h in the high/high category was −1.63 °C, whereas for those in the low/low category it was −0.72 °C. These differences were reduced at 0500 h, with a high/high mean $dT_a$ of −1.02 and a low/low mean of −0.21. The low/low values at 0500 h were clustered around areas with little vegetation and surrounding rooftops, a spatial pattern that was reduced around asphalt but extended to the exposed soil land covers at 1700 h.

## Surface temperature differences and surface covers

Increased vegetation in the LA scenario showed significant mean surface temperature reductions from RV conditions for the model simulation period ($dT_s$=LA $T_s$ - RV $T_s$, Fig. 4). There were insignificant variations in $dT_s$ during the first 2–3 simulation hours (which could be attributed to model spin-up) but significant cooling for all surfaces commenced from noon and was most pronounced during late afternoon. Similar to Fig. 3, vegetated and pervious surfaces decreased in mean $dT_s$, but the magnitude of surface cooling for all types of surfaces was much larger compared to near-surface ambient temperatures (e.g. −8.2 °C vs. −1.9 °C for tree surfaces at 1500 h, see Fig. 4). The greater surface cooling suggested a strong influence of vegetated canopy shading that reduced direct insolation.

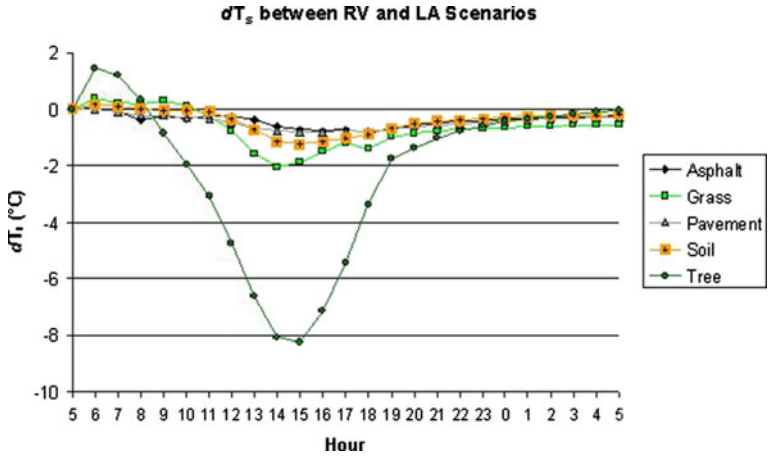


**Fig. 4** 24-hour profile of mean differences in surface temperature ($dT_s$) by surface cover between RV and LA scenarios

Magnitudes of nocturnal mean $dT_s$, however, were smaller for all surfaces compared to their corresponding values of *dTa.*

The statistical and spatial distributions of absolute surface temperatures at 1700 h varied considerably among the RV and LA scenarios. Linked-window maps of surface temperature highlight the sharp differences in the statistical distribution and correlation with surface covers in the EV (Online Resource 3) and LA (Online Resource 4) scenarios. Histogram bins for both RV and LA results were grouped into three distinct distributions observable in the RV and LA histograms (Online Resources 3b and 4b). $T_s$ observations in increasing order of magnitude were color coded blue, yellow, and red and linked in GIS to a surface cover map overlay to highlight surface temperature differences. In both histograms, observations coded in blue, yellow, and red generally corresponded to vegetated, bare soil, and impervious surface covers, respectively. There were, however, deviations from this pattern which suggested a cooling effect especially pronounced in the LA scenario. Areas in the low range of the distribution (blue, 25.3 °C>= $T_s$<37.6 °C) in the RV scenario were located at or near modeling cells with tree canopy surface covers. In the LA scenario, the low range of temperatures expanded to cells at or near canopied cells, creating a cooling effect that extended to the impervious surface covers surrounding trees (Online Resource 4). Although impervious covers had the highest $T_s$ values in both distributions, asphalt close to tree canopies in the LA scenario (west and central areas of the park) belonged to the (yellow) midrange, indicating net reductions in surface temperature.

Although the surface temperatures were very high even in the low range (< 37.6 °C), the linked-window displays illustrate the potential for $T_s$ reductions if the RV scenario were transformed into the LA vegetation conditions: 1452 cells in the blue bin in RV increased to 1827 in the LA scenario. Conversely, the number of cells in the high range (> 39.7 °C), decreased from 4212 (RV) to 3825 (LA), suggesting that surface temperatures in and around cells with tree canopies were reduced due to a cooling effect (Online Resource 4a).

## Discussion and conclusions

Our analyses of modeled air and surface temperatures showed that increasing vegetation in parks can mitigate local effects of the UHI by creating localized PCIs where extreme temperatures are lowered, sometimes significantly. The LISA analysis of air temperature indicated that for hours of typical daily minimum (0500 h) and maximum (1700 h) $T_a$, the largest reductions (i.e., most negative $dT_a$ values) for the Landscape Architecture (LA) park scenario compared to the Representative Vegetation (RV) scenario (Online Resources 2 and 1) were spatially clustered around canopied vegetation and immediately adjacent to non-vegetated surfaces. Conversely, the smaller temperature reductions (i.e., least negative $dT_a$ values) were clustered around areas with exposed soil, asphalt, or other impervious surfaces that were not immediately contiguous to vegetative surfaces. The 24-hour profile of mean $T_a$ also showed the significant cooling effects of vegetation in the LA scenario through shading and transpirational cooling. These negative $dT_a$ values suggested a distinct PCI effect that we estimated to have the potential to cool the air (underneath or surrounded by canopied vegetation) by as much as 1.9 °C during the warmest time of the day.

The greatest reductions in surface temperatures between the LA and the RV scenarios occurred in grass (1400 h) and tree surface covers (1500 h), with mean $dT_s$=−2.1 °C and −8.2 °C, respectively. A spillover effect of vegetation, similar to that observed in the diurnal profile for $T_a$, occurred in $T_s$ values for impervious covers (asphalt and pavement), which registered mean $dT_s$=−0.8 °C. The linked window

analysis of $T_s$ (Online Resources 3 and 4) illustrated the adjacent cooling effect of vegetation upon non-vegetated surfaces, namely that clusters of canopied vegetation can help cool impervious surfaces.

Anthropogenic changes of natural land covers into heat-retaining surfaces like roofs, pavement, or asphalt (e.g., through new housing development) are known to be related to increases in temperature (Brazel et al. 2007). $T_s$ data are important in comparisons with remotely-sensed land cover data, usually in studies that evaluate the role of surface material changes in heat island mitigation. In our study, the degree of coupling between these two variables was dependent on factors such as scale, land cover type and atmospheric stability. Although air and surface temperatures are usually correlated under low wind speeds, atmospheric turbulence conditions can decouple surface-air temperatures (Stoll and Brazel 1992). In our study, however, simulated values of $T_s$ and $T_a$ correlated well, ($r$=0.69 for the LA scenario; $r$=0.75 for EV at 1700 h) largely due to the small geographic scale of the study area, and atmospheric stability during our modeling period (wind speed=3.58 m/s, see Table 3).

Comparison of the RV and proposed LA scenarios demonstrated that increasing vegetation is one strategy through which extreme heat can be mitigated in arid cities. Providing adequate green spaces in the inner city is a critical component of UHI mitigation during the hot season, especially during EHEs. This is made difficult, however, by ongoing contestations over adequate urban amenities like parks and the resources necessary to provide them (e.g., water, tax dollars, local government will, regular maintenance). Contestations about the allocation of resources resonate with claims of environmental injustice that "ecologies of fear" (Brownlow 2006) often arise in neglected green spaces as legacies of environmental and racial discrimination, inner-city decay, and a continuing urban planning focus on fringe development. Indeed, in Phoenix, Guhathakurta and Wichert (1998) have shown that although inner-city areas bear higher property tax burdens in comparison with the suburbs, the former receive significantly fewer tax dollars than the latter for parks, recreation, and water supply.

Minority and low-income communities are increasingly addressing such disparities by demanding more equitable distribution of urban amenities, such as parks and clean air. Their desire for more vegetation is often framed as a means for neighborhood beautification and improving the quality of parks as community anchors and points of pride. Parks in low-income (but not exclusively) Hispanic communities often are the only available public gathering places that also embody a historical and cultural sense of place due to ties of past and present residents. Disparities in the distribution of fiscal and natural resources also translate into inequalities in ecosystem services, such as shading and transpirational cooling, that have significant and measurable outcomes in UHI impacts (Heisler et al. 1995; Perkins et al. 2004). Although the community in this study did not frame their arguments for park improvement explicitly around the heat mitigation benefits demonstrated in our research, this service may become more important in the future as the trend of increasing temperatures continues.

Green spaces can provide social, cultural, and—more directly for extreme heat mitigation—human health and ecological benefits (Boone et al. 2009; Spronken-Smith and Oke 1998; Wolch et al. 2005). Microclimate modeling combined with localized knowledge of vegetation, GIS, and spatial autocorrelation helps to close existing gaps in understanding ecological relationships between vegetation and extreme heat mitigation in low-income, urban core neighborhoods. One direction for future research is to validate modeled results with observed atmospheric data, which is a component of atmospheric modeling we did not engage in our scenario-building. Future research should investigate seasonal variability of the UHI, not only

during EHE episodes but also during the cold season because the increased heat storage characteristic of the UHI can potentially mitigate the intensity of winters.

One aspect of extreme heat not addressed directly in our study was human thermal comfort. ENVI-Met can estimate Median Radiant Temperature (MRT) and Predicted Mean Vote (PMV), two indicators of human thermal comfort. BOT World, an agent-based modeling system for thermal comfort is also available with ENVI-Met. Additionally, Matzarakis et al. (2010) have implemented RayMan, a bodily-scale human-energy balance model. Understanding human thermal comfort requires further research and input data to implement at the microscale in complex urban environments such as our study area. For example, assessing thermal comfort in arid climates requires evaluation of radiant heat flux because it is a more important determinant of human thermal comfort than air temperature (Shashua-Bar et al. 2010b; Pearlmutter et al. 2006).

Water consumption for vegetation in Phoenix plays a critical role in urban planning and policy-making because tradeoffs in using water and energy to produce ecosystem services are unavoidable in a water-scarce region. Water consumption for outdoor landscaping in Phoenix accounts for roughly 45 to 70% of total residential water use (Gober et al. 2009). Generally, there is higher irrigation in landscapes dominated by turf grass than landscapes comprised of desert-adapted trees and shrubs (Martin and Stabler 2004) but water consumption for irrigation is highly variable. For example, Martin and Stabler (2002) reported that the range of supplemental water for residential landscape irrigation in Phoenix can vary from 0 to 233 L/m$^2$/month. These data suggest that microclimate cooling created by localized PCIs might require substantial inputs of water resources to irrigate—especially turf grass—underscoring the paradox of conflicting ecosystem services in arid regions of water conservation and UHI mitigation through evapotranspirational cooling (Jenerette et al. 2011). Vegetation scenarios focused on microscale UHI mitigation in arid cities should explore the spatial and temporal variability of irrigation in relation to cooling. ENVI-Met's treatment of irrigation conditions is currently limited to soil moisture and temperature variables differentiated vertically among three layers, but not horizontally among modeling cells. Thus the model did not allow us to explore cooling differences from irrigation regimes among land covers.

Another important point to consider is the potential tradeoff between irrigation water and UHI mitigation, which suggests the potential for greatest temperature reductions exists in neighborhoods with small amounts of vegetation (Gober et al. 2009) such as our low-income study area. It is also of interest to evaluate the cost-benefit ratio of water application vs. temperature reductions (see Jenerette et al. 2011). In this regard, Shashua-Bar et al. (2010a) have suggested that the reconciliation of these conflicting ecosystem services might best be realized through landscape design modalities consisting of shade trees alone, while Zhou et al. (2011) have found that the composition and configuration of vegetated landscape has significant impacts on UHI mitigation.

In this study, we applied ENVI-Met to assess the potential benefits of the LA scenario to the surrounding microclimate. ENVI-Met allows researchers to model the climate of a spatially discrete urban area (i.e. individual buildings, gardens, green spaces, canals etc.) and to test the effects of architectural and planning design scenarios on microclimates. ENVI-Met has been applied to scenario-testing in other cities at a building and neighborhood spatial scale (e.g., Emmanuel and Fernando 2007), and is one of the few urban computational fluid dynamics models that is relatively user-friendly for planners and architects. It has the capabilities to model several aspects of microscale urban climates (e.g. temperature, wind field and thermal comfort variations) that are not possible with other numerical or scale models. Like all models, however, ENVI-Met has its limitations. For

instance, the inability of the model to account for albedo variations among buildings within its model domain (i.e. all modeled structures have the same assigned wall and roof albedo magnitude) possibly affects its accuracy in heterogeneous urban areas with different wall/roof colors and materials (see Chow et al. 2011 for further discussion of model limitations). Despite such limitations, the model can still be a very useful tool for urban planners, landscape architects, and other practitioners, provided that users are cognizant of the model's limitations and have initialized the model with accurate parameters (e.g. local vegetation and soil conditions).

This study contributed to a microscale understanding of energy fluxes among vegetated, non-vegetated, and impervious surfaces in an arid urban area that is demonstrably getting hotter. Through the scenario building exercise presented here, our research engaged in an interdisciplinary effort to understand the localized impacts of climate change and to inform strategies to mitigate the effects of the UHI through the creation of park cool islands in low-income, inner-city neighborhoods.

**Acknowledgments** The work presented here is funded by the National Science Foundation under Grant No. GEO-0816168, Urban Vulnerability to Climate Change. The authors thank Ben Ruddell at the Arizona State University College of Technology and Innovation for comments on an early manuscript, Nancy Selover, Arizona State Climatologist, for providing PRISMS meteorological station data, and Juan Brenes-García, SBD Studio for advice on landscape design. We also thank the editor and anonymous reviewers for helpful commentary that improved this article. The authors accept responsibility, however, for our ideas, results, and interpretations.

## References

Anderson GB, Bell ML (2011) Heat waves in the United States: mortality risk during heat waves and effect modification by heat wave characteristics in 43 U.S. communities. Environ Health Perspect 119(2):210–218

Anselin L (1995) Local indicators of spatial association - LISA. Geogr Anal 27:93–115

ASTER SP (2010) Characteristics of ASTER sensor. http://www.science.aster.ersdac.or.jp/en/about_aster/sensor/tokutyou.html. Accessed 11 July 2012

Balling RC, Brazel SW (1987) The impact of rapid urbanization on pan evaporation in Phoenix, Arizona. J Climatol 7:593–597

Barradas VL, Tejeda-Martinez A, Jauregui E (1999) Energy balance measurements in a suburban vegetated area in Mexico City. Atmos Environ 33:4109–4113

Boone C, Buckley G, Grove J, Sister C (2009) Parks and people: an environmental justice inquiry in Baltimore, Maryland. Ann Assoc Am Geogr 99:767–787

Brazel A, Selover N, Vose R, Heisler G (2000) The tale of two climates - Baltimore and Phoenix urban LTER sites. Clim Res 15:123–135

Brazel A, Gober P, Lee SJ, Grossman-Clarke S, Zehnder J, Hedquist B, Comparri B (2007) Determinants of changes in the regional urban heat island in metropolitan Phoenix (Arizona, USA) between 1990 and 2004. Clim Res 33:171–182

Brownlow A (2006) An archaeology of fear and environmental change in Philadelphia. Geoforum 37(2):227–245

Bruse M, Fleer H (1998) Simulating surface-plant-air interactions inside urban environments with a three dimensional numerical model. Environ Model Software 13:373–384

Buyantuyev A, Wu J (2012) Urbanization diversifies land surface phenology in arid environments: interactions among vegetation, climatic variation, and land use pattern in the Phoenix metropolitan region, USA. Landsc Urban Plan 105:149–159

Byrne J, Wolch J, Zhang J (2009) Planning for environmental justice in an urban national park. J Environ Plan Manag 52:365–392

Chow WTL, Pope RL, Martin CA, Brazel AJ (2011) Observing and modeling the nocturnal park cool island of an arid city: horizontal and vertical impacts. Theor Appl Climatol 103:197–211

Currie B, Bass B (2008) Estimates of air pollution mitigation with green plants and green roofs using the UFORE model. Urban Ecosyst 11:409–422

de Groot RS, Alkemade R, Braat L, Hein L, Willeman L (2010) Challenges in integrating the concept of ecosystem services and values in landscape planning, management and decision making. Ecol Complex 7:260–272

de Smith MJ, Goodchild MF, Longley PA (2007) Geospatial Analysis. Troubador Publishing Ltd

Diffenbaugh N, Pal J, Trapp R, Giorgi F (2005) Fine-scale processes regulate the response of extreme events to global climate change. Proc Natl Acad Sci USA 102:15774–15778

Dooling S, Simon G, Yocom K (2006) Place-based urban ecology: a century of park planning in Seattle. Urban Ecosyst 9:299–321

Emmanuel R, Fernando H (2007) Urban heat islands in humid and arid climates: role of urban form and thermal properties in Colombo, Sri Lanka and Phoenix, USA. Clim Res 34:241–251

EPA (2011) Natural Disasters and Weather Emergencies: Extreme Heat. http://www.epa.gov/naturalevents/extremeheat.html. Accessed 11 July 2012

Garcia-Cueto OR, Jauregui-Ostos E, Toudert D, Tejeda-Martinez A (2007) Detection of the urban heat island in Mexicali, B. C., Mexico and its relationship with land use. Atmosfera 20:111–131

Gober P, Brazel A, Quay R, Myint S, Grossman-Clarke S, Miller A, Rossi S (2009) Using watered landscapes to manipulate urban heat island effects: how much water will it take to cool Phoenix? J Am Plann Assoc 76:109–121

Grimmond C, Souch C, Hubble M (1996) Influence of tree cover on summertime surface energy balance fluxes, San Gabriel Valley, Los Angeles. Clim Res 6:45–57

Grossman-Clarke S, Zehnder JA, Stefanov WL, Liu Y, Zoldak MA (2005) Urban modifications in a mesoscale meteorological model and the effects on near-surface variables in an arid metropolitan region. J Appl Meteorol 44:1281–1297

Guhathakurta S, Wichert M (1998) Who pays for growth in the city of Phoenix? An equity-based perspective on suburbanization. Urban Aff Rev 33:813–838

Harlan SL, Brazel AJ, Prashad L, Stefanov WL, Larsen L (2006) Neighborhood microclimates and vulnerability to heat stress. Soc Sci Med 63:2847–2863

Hedquist BC, Di Sabatino S, Fernando HJS, Brazel AJ (2009) Results from the Phoenix Arizona Urban Heat Island Experiment. The seventh International Conference on Urban Climate. 29 June – 3 July 2009, Yokohama, Japan. http://www.ide.titech.ac.jp/~icuc7/extended_abstracts/pdf/384812-1-090518233339-002.pdf. Accessed 14 Dec 2012

Heisler GM, Grant RH, Grimmond S, Souch C (1995) Urban forests—cooling our communities? In: Kollin C, Barratt M (eds) Proceedings: 7th national urban forest conference. American Forests. Washington, DC, pp 31–34. http://www.fs.fed.us/psw/programs/uesd/uep/products/cufr_57_EM95_25.PDF. Accessed 14 Dec 2012

Hill T, Polsky C (2007) Development and drought in suburbia: a mixed methods rapid assessment of vulnerability to drought in rainy Massachusetts. Glob Environ Chang Part B Environ Hazards 7:291–301

Huttner S, Bruse M, Dostal P (2008) Using ENVI-met to simulate the impact of global warming on the microclimate in central European cities. In: Mayer H, Matzarakis A (eds) Berichte des Meteorologischen Instituts der Albert-Ludwigs-Universität Freiburg Nr. 18: 5th Japanese-German Meeting on Urban Climatology, pp 307–312. http://www.envi-met.com/documents/papers/Huttner_etal_2008.pdf. Accessed 14 Dec 2012

Intergovernmental Panel on Climate Change (IPCC) (2007) Climate Change 2007: Synthesis Report. http://www.ipcc.ch/publications_and_data/publications_ipcc_fourth_assessment_report_synthesis_report.htm. Accessed 11 July 2012

Jenerette GD, Harlan SL, Brazel A, Jones N, Larsen L, Stefanov WL (2007) Regional relationships between surface temperature, vegetation, and human settlement in a rapidly urbanizing ecosystem. Landsc Ecol 22:353–365

Jenerette GD, Harlan SL, Stefanov WL, Martin CA (2011) Ecosystem services and urban heat riskscape moderation: water, green spaces, and social inequality in Phoenix, USA. Ecol Appl 21:2637–2651

Jennings V, Johnson Gaither C, Schulterbrandt Gragg R (2012) Promoting environmental justice through urban green space access: a synopsis. Environ Justice 5:1–7

Lahme E, Bruse M (2003) Microclimatic effects of a small urban park in densely built-up areas: measurements and model simulations. Fifth International Conference on Urban Climate(ICUC5) Lodz, 1–5 September 2003. http://www.envi-met.com/documents/papers/park2003.pdf. Accessed 14 Dec 2012

Lalic B, Mihailovic DT (2004) An empirical relation describing leaf-area density inside the forest for environmental modeling. J Appl Meteorol 43:641–645

Lowry W (1967) The climate of cities. Sci Am 217:15–23

Martin CA (2009) Virtual Library of Phoenix Landscape Plants. http://www.public.asu.edu/~camartin/Martin%20landscape%20plant%20library.htm. Accessed 11 July 2012

Martin CA, Stabler LB (2002) Plant gas exchange and water status in urban desert landscapes. J Arid Environ 51:235–254

Martin CA, Stabler LB (2004) Urban horticultural ecology: interactions between plants, people and the physical environment. Acta Horticult 639:97–101
Martin CA, Warren PS, Kinzig AP (2004) Neighborhood socioeconomic status is a useful predictor of perennial landscape vegetation in residential neighborhoods and embedded small parks of Phoenix, Arizona. Landsc Urban Plan 69:355–368
Matzarakis A, Rutz F, Mayer H (2010) Modelling radiation fluxes in simple and complex environments: basics of the RayMan model. Int J Biometeorol 54:131–139
Meehl G, Tebaldi C (2004) More intense, more frequent, and longer lasting heat waves in the 21st century. Science 305:994–997
Mills G (2006) Progress toward sustainable settlements: a role for urban climatology. Theor Appl Climatol 84:69–76
Oke TR (1989) The micrometeorology of the urban forest. Philos Trans R Soc B Biol Sci 324:335–349
Oke TR (1997) The changing climatic environments: urban climates and global environmental change. Routledge, London
Ozkeresteci I, Crewe K, Brazel AJ, Bruse M (2003) Use and evaluation of the ENVI-Met model for environmental design and planning: an experiment of linear parks. Proceedings of the 21st International Cartographic Conference. 10–16 August 2003, Durban, South Africa. http://icaci.org/files/documents/ICC_proceedings/ICC2003/Papers/516.pdf. Accessed 18 Dec 2012
Payne-Sturges D, Gee GC, Crowder K, Hurley BJ, Lee C, Morello-Frosch R, Rosenbaum A, Schulz A, Wells C, Woodruff T, Zenich H (2006) Workshop summary: connecting social and environmental factors to measure and track environmental health disparities. Environ Res 102:146–153
Pearlmutter D, Berliner P, Shaviv E (2006) Physical modeling of pedestrian energy exchange within the urban canopy. Build Environ 41:783–795
Perkins H, Heynen N, Wilson J (2004) Inequitable access to urban reforestation: the impact of urban political economy on housing tenure and urban forests. Cities 21:291–299
Robaa S (2003) Urban-suburban/rural differences over greater Cairo, Egypt. Atmósfera 16(3):157–171. http://www.ejournal.unam.mx/atm/Vol16-3/ATM16303.pdf. Accessed 18 Dec 2012
Rosheidat A, Hoffman D, Bryan H (2008) Visualizing pedestrian comfort using ENVI-Met. Third National Conference of IBPSA-USA, July 30 – August 1, 2008, Berkeley, California. http://www.ibpsa.us/simbuild2008/technical_sessions/SB08-DOC-TS10-2-Rosheidat.pdf. Accessed 18 Dec 2012
Roth M (2002) Effects of cities on local climates. Proceedings of Workshop of IGES/APN Mega-City Project. Rihga Royal Hotel Kokura, Kitakyushu Japan, January 2002. http://enviroscope.iges.or.jp/contents/13/data/PDF/08-1(Roth).pdf. Accessed 18 Dec 2012
Ruddell DM, Harlan SL, Grossman-Clarke S, Buyantuyev A (2010) Risk and exposure to extreme heat in microclimates of Phoenix, AZ. In: Showalter PS, Lu Y (eds) Geospatial techniques in urban hazard and disaster research. Springer, New York, pp 179–202
Shashua-Bar L, Potchter O, Bitan A, Boltansky D, Yaakov Y (2010a) Microclimate modelling of street tree species effects within the varied urban morphology in the Mediterranean city of Tel Aviv, Israel. Int J Climatol 30:44–57
Shashua-Bar L, Pearlmutter D, Erell E (2010b) The influence of trees and grass on outdoor thermal comfort in a hot-arid environment. Int J Climatol 31(6):1498–1506
Spronken-Smith RA, Oke TR (1998) The thermal regime of urban parks in two cities with different summer climates. Int J Remote Sens 19(11):2085–2104
Stabler LB, Martin CA, Brazel AJ (2005) Microclimates in a desert city were related to land use and vegetation index. Urban For Urban Green 3:137–147
Stoll M, Brazel AJ (1992) Surface-air temperature relationships in the urban environment of Phoenix, Arizona. Phys Geogr 13:160–179
USD of A (2007) National Agriculture Imagery Program (NAIP). Geospatial Data Gateway. http://datagateway.nrcs.usda.gov/. Accessed 11 July 2012
Voogt JA, Oke TR (2003) Thermal remote sensing of urban climates. Remote Sens Environ 86:370–384
Walker J, Blaschke T (2008) Object-based land-cover classification for the Phoenix metropolitan area: optimization vs. transportability. Int J Remote Sens 29:2021–2040
Wilson SM (2009) An ecologic framework to study and address environmental justice and community health issues. Environ Justice 2:15–24
Wolch J, Wilson JP, Fehrenbach J (2005) Parks and park funding in Los Angeles: an equity mapping analysis. Urban Geogr 26:4–35
Wolf J, Adger WN, Lorenzoni I, Abrahamson V, Raine R (2010) Social capital, individual responses to heat waves and climate change adaptation: an empirical study of two UK cities. Glob Environ Chang 20:44–52
Zhou W, Huang G, Cadenasso ML (2011) Does spatial configuration matter? Understanding the effects of land cover pattern on land surface temperature in urban landscapes. Landsc Urban Plan 102:54–63